Enhanced Antitumor Immunity in Mice Deficient in CD69

Enric Esplugues,[1] David Sancho,[2] Javier Vega-Ramos,[1] Carlos Martínez-A,[3] Uta Syrbe,[4] Alf Hamann,[4] Pablo Engel,[5] Francisco Sánchez-Madrid,[2] and Pilar Lauzurica[1]

[1]*Departamento de Fisiología, Universidad de Barcelona, Barcelona 08080, Spain*
[2]*Servicio de Immunología, Hospital de la Princesa, Madrid 28006, Spain*
[3]*Department of Immunology and Oncology, Centro Nacional de Biotecnología, Spanish Council for Scientific Research-UAM, Madrid 28006, Spain*
[4]*Experimentelle Rheumatologie, Medizinische Klinik, Charite, Humboldt-Universitat Berlin and Deutsches Rheumaforschungszentrum, Berlin 10117, Germany*
[5]*Immunology Unit, Department of Cellular Biology and Pathology, University of Barcelona Medical School, Institut d'Investigacions Biomediques August Pi y Sunyer, Barcelona 08080, Spain*

Abstract

We investigated the in vivo role of CD69 by analyzing the susceptibility of CD69−/− mice to tumors. CD69−/− mice challenged with MHC class I^- tumors (RMA-S and RM-1) showed greatly reduced tumor growth and prolonged survival compared with wild-type (WT) mice. The enhanced anti–tumor response was NK cell and T lymphocyte–mediated, and was due, at least in part, to an increase in local lymphocytes. Resistance of CD69−/− mice to MHC class I^- tumor growth was also associated with increased production of the chemokine MCP-1, diminished TGF-β production, and decreased lymphocyte apoptosis. Moreover, the in vivo blockade of TGF-β in WT mice resulted in enhanced anti–tumor response. In addition, CD69 engagement induced NK and T cell production of TGF-β, directly linking CD69 signaling to TGF-β regulation. Furthermore, anti-CD69 antibody treatment in WT mice induced a specific down-regulation in CD69 expression that resulted in augmented anti–tumor response. These data unmask a novel role for CD69 as a negative regulator of anti–tumor responses and show the possibility of a novel approach for the therapy of tumors.

Key words: cytokines • homeostasis • apoptosis

Introduction

AIM/CD69 is the earliest activation cell surface receptor on leukocytes. CD69 is a C-type lectin, disulfide-linked homodimer (24 kD), type II protein (1). The genetic and biochemical characteristics of mouse CD69 are very similar to its human homologue. CD69 is constitutively expressed by platelets, mature thymocytes, bone marrow myeloid, and lymphoid precursors. CD69 is not detected in peripheral blood lymphocytes, but it is expressed by small subsets of T and B cells in peripheral lymphoid tissues (2, 3). Nevertheless, CD69 does not appear to be required for the development of any bone marrow cell lineage because nearly normal hematopoietic cell development and T cell maturation occur in CD69−/− mice. Only minor alterations are observed in B cell development in these mice, with the $B220^{hi}IgM^{neg}$ bone marrow pre–B cell compartment slightly augmented (4).

CD69 expression is induced by cytokine stimulation on leukocytes (5, 6). Accordingly, $CD69^+$ T lymphocytes are detected in cell infiltrates of various chronic inflammatory diseases (7). Moreover, CD69 is expressed by activated T, B, and NK cells and monocytes in LPS-treated mice (8). On the other hand, the intracellular signals induced through CD69 result in cytokine and cytokine receptor synthesis in T cells (3, 9–12). CD69 expression is induced on NK cells by IL-2 (5), IFN-α (13), cross-linking of FcγRIII, and activators of PKC (14). Furthermore, stimulation of activated NK cells with anti-CD69 antibodies stimulates cytolytic activity (15).

Chemokines and cytokines control leukocyte attraction and activation, whereby regulating immune homeostasis.

Address correspondence to Pilar Lauzurica, Departmento de Fisiología, Universidad de Barcelona, Avenida Diagonal, 645, Barcelona 08080 Spain. Phone: 34-93-403-5924; Fax: 34-93-411-0358; E-mail: lauzu@porthos.bio.ub.es

 J. Exp. Med. © The Rockefeller University Press • 0022-1007/2003/05/1093/14 $8.00
Volume 197, Number 9, May 5, 2003 1093–1106
http://www.jem.org/cgi/doi/10.1084/jem.20021337

Monocyte chemotactic protein-1 (MCP-1)* chemokine is produced early after exposure to immune stimuli (16), and has been implicated in enhancing lymphocyte migration and cytotoxicity (17). Furthermore, animals that lack MCP-1 show diminished T cell responses (18). TGF-β prevents and/or suppresses inflammatory responses, regulating production of proinflammatory cytokines (for review see reference 19). Several clinical and experimental observations suggest that CD69 expression is regulated, at least in part, by these cytokines. In this regard, it has been described previously that TGF-β down-regulates the expression of CD69 in factor VIII–treated patients (19a). In addition, tumor patients treated with proinflammatory cytokines show increased levels of immunosuppressive cytokines (e.g., IL-10 and TGF-β) and decreased tumor infiltration by $CD69^+$ lymphocytes (20).

The immune response against tumors involves the combined action of humoral and cellular mechanisms, in which macrophages, cytotoxic T, and NK lymphocytes play a central role. Tumor models have provided useful tools to dissect complex anti–tumor immune responses (21, 22). Here, we analyzed the influence of CD69 deficiency on the anti–tumor response in CD69−/− mice. CD69−/− mice showed an enhanced NK cell–dependent response that leads to a higher protection and rejection of MHC class I^- tumor cells compared with wild-type (WT) mice. This potent anti–tumor response was dependent on the tumor–host microenvironment, correlating with a diminished TGF-β production and an increase in inflammatory cytokines and MCP-1, and was associated with increased recruitment of lymphoid effector cells and diminished apoptosis. In addition, the in vivo blockade of TGF-β in WT mice increased anti–tumor response. Moreover, we found that cross-linking of CD69 induced TGF-β production, directly linking CD69 signaling to TGF-β regulation. Furthermore, down-modulation of CD69 expression induced in WT mice through anti-CD69 antibody treatment produced increased anti–tumor response. These findings reveal a novel role for CD69 as a negative regulator of immune homeostasis through TGF-β modulation.

Materials and Methods

Mice. Mice were bred at the Centro Nacional de Biotecnología under specific pathogen-free conditions and at the University of Barcelona in a conventional facility. All experiments were performed using mice on a C57BL/6 genetic background except in in vivo homing assays and in in vivo tumor challenges in RAG2−/−, which were performed in BALB/c mice. CD69−/− mice were backcrossed on C57BL/6 or BALB/c background at least nine times. C57BL/6, BALB/c WT, and gene-targeted CD69−/− mice (4) were 6–12 wk old, and littermate or age-matched litters, whose parents were littermates, were used as controls. C57BL/6, BALB/c, and RAG2−/− mice were purchased from Jackson ImmunoResearch Laboratories. For the generation of RAG2−/− × CD69−/− mice, the status of the RAG2 locus was followed by assaying blood for $CD3^+$ cells by FACS®. Genotyping of the CD69 locus was performed by polymerase chain reaction as described previously (4). All procedures involving animals and their care were approved by the Ethics Committee of the University of Barcelona and were conducted according to institutional guidelines that are in compliance with national (Generalitat de Catalunya decree 214/1997, DOGC 2450) and international (Guide for the Care and Use of Laboratory Animals, National Institutes of Health, 85–23, 1985) laws and policies.

Cell Culture. The RM-1 prostate carcinoma ($H\text{-}2^b$, a gift from Dr. T. Thompson [Baylor College of Medicine, Houston, TX]), YAC-1 ($H\text{-}2^a$), RMA ($H\text{-}2^b$) lymphoma cell lines, RMA-S ($H\text{-}2^b$) mutant lymphoma cells (derived from Rauscher virus–induced murine cell line RBL-5 and defective for peptide loading of MHC class I molecules), and 300.19 pre–B cells were cultured in RPMI 1640 medium supplemented with 10% heat-inactivated FCS, 2 mm L-glutamine, 100 U/ml penicillin, and 100 μg/ml streptomycin (GIBCO BRL) at 37°C, 5% CO_2.

Cell Isolation. Peritoneal macrophages were isolated by plastic adhesion, and further subset purification was performed with magnetic beads (Miltenyi Biotec) and specific biotin-conjugated Ab (BD Biosciences), yielding ~98% cell purity.

Tumor Control In Vivo. Tumor cells (RMA, RMA-S, or RM-1) in 0.2 ml PBS were injected intraperitoneally or subcutaneously in untreated WT and CD69−/− mice, and in antibody-depleted mice, as indicated. In experiments performed with NK cell–depleted mice, animals were injected intraperitoneally with 100 μl rabbit anti–asialo-GM-1 (Wako Chemicals) 1 d before tumor inoculation, and at days +2 and +4 after tumor challenge. Mice were treated for lymphocyte T $CD4^+$ depletion on day −1 (before tumor challenge), and at days +2 and +4 after tumor inoculation with either GK1.5 anti-CD4 or isotype control mAbs (100 μl/injection). Mice were observed by monitoring body weight daily for tumor ascites development for 12 wk. Mice were killed, for ethical reasons, when the body weight had increased by 25%, corresponding to note obvious signs of irreversible tumor growth, and when the animals became moribund.

RM-1 Lung Colonization. 10^4 RM-1 cells suspended in 100 μl PBS were injected into the tail vein of CD69−/− and WT mice. Mice were killed 14 d later, the lungs were removed and fixed in 4% paraformaldehyde solution, and individual surface lung metastases were counted with the aid of a dissecting microscope.

Flow Cytometry. Spleen and peritoneal exudate cells (10^6) were first preincubated with a blocking solution (PBS with 5% heat-inactivated FCS, 15% heat-inactivated rabbit serum, 0.02% sodium azide and 2.4G2 mAb) to avoid binding of Abs to Fcγ receptors. Cells were stained for 30 min on ice with FITC- or PE-conjugated antibodies or with biotinylated antibodies followed by streptavidin-FITC or -PE (Southern Biotechnology Associates, Inc.) The following antibodies were used: anti-DX5 (DX5), -2B4 (2B4), CD2 (RM2–5), -CD3 (145–2C11), -B220/CD45 (RA3–6B2), -CD4 (GK1.5), -CD5 (53–7.3), -CD8 (53–6.7), -CD11b (M1/70), -Ly6G (RB6–8C5), IgM (G155–228), and -CD69 (H1.2F3; all from BD Biosciences) and IgD (Southern Biotechnology Associates, Inc.; 11–26). Finally, cells were washed and analyzed on a FACSCalibur™ flow cytometer (Becton Dickinson), counting 10^4 live cells and using CELLQuest™ software (Becton Dickinson). The number of cells migrating to the peritoneum was determined with a Multisizer II (Beckman Coulter).

IL-2–activated NK Cells. Purified spleen NK cells were obtained with the CELLection Biotin Binder Kit (Dynal) and biotinylated anti-DX5 antibody, according to manufacturer's instruc-

*Abbreviations used in this paper: MCP-1, monocyte chemotactic protein-1; PI, propidium iodide; RPA, RNase protection assay; WT, wild-type.

tions. In brief, viable single cell suspensions were incubated (1 h at 37°C) on polystyrene tissue culture dishes (Becton Dickinson). Nonadherent spleen cells were incubated (15 min at 4°C) with biotinylated anti-DX5 antibody, washed twice, and CELLection biotin magnetic Dynabeads (10^7 magnetic beads per 10^6 cells) were added to capture antibody-coated cells. Cell purity was always >98% $DX5^+$. NK cells were cultured in complete medium with 20% inactivated FCS, alone, or with 1,000 UI/ml human rIL-2 (72 h).

^{51}Cr Release Assays. Direct NK cell cytotoxic activity was assessed by a standard ^{51}Cr release assay. In all experiments, 5×10^3 sodium [^{51}Cr]chromate-labeled YAC-1 target cells were mixed with effector cells at the ratios indicated (4 h at 37°C). Spontaneous ^{51}Cr release was determined by incubating target cells with medium alone; maximum release was determined by adding TritonX100 at a final concentration of 2.5%. The percentage of specific lysis was calculated as percentage specific lysis = ([sample cpm − spontaneous cpm]/[maximal cpm − spontaneous cpm]) × 100. Spontaneous ^{51}Cr release was always <10%, and all experiments were performed in triplicate.

In Vivo Homing Assays. Lymphocytes were isolated from single cell suspensions of lymph nodes, spleen, and other organs. For isolation of $CD4^+$ T lymphocytes, cells were incubated with anti-CD8 and anti–MAC-1 mAb, followed by two panning steps on petri dishes coated with a rabbit anti–mouse/rat IgG (DakoCytomation) at 4°C. The average purity of $CD4^+$ cells was >95%, as determined by flow cytometry analysis.

The migration of radioactively labeled lymphocytes was analyzed as described previously (38). In brief, cells were labeled with 20 μCi/ml sodium [^{51}Cr]chromate (1 h at 37°C). Dead cells were removed by centrifugation on a density cushion (Nycodenz). $0.5–2 \times 10^6$ cells suspended in 0.3 ml PBS were injected into the tail vein. Mice were killed 1 or 24 h later, and the distribution of the radioactivity in different organs and the remaining body was measured.

Cell Death Assays. Splenocytes (4×10^6 cells/ml) from challenge mice (3 d with 10^5 RM-1) were cultured in 24-well plates (Costar), and cell death was assayed 24 h after the initiation of culture. Cell cycle was monitored, cells were stained with propidium iodide (PI), and apoptosis was determined by flow cytometric analysis on an XL cytometer (Beckman Coulter). Data are expressed as mean ± SE ($n = 9$). Caspase-3 activity was assayed at 48 h after initiation of culture by incubation with the PhiPhiLux-G1D2 substrate solution (OncoImmunin) according to the manufacturer's protocol. Flow cytometric analysis was performed within 60 min of the end of the incubation period with an XL cytometer. Peritoneal cells (10^6) from untreated mice were cultured in 24-well plates, and cell death was assessed, at indicated time points, by PI staining. PI^+-stained samples were considered apoptotic cells.

RNase Protection Assay (RPA) and Quantitative Real-time RT-PCR Analyses. Total RNA was extracted from unfractionated peritoneal cells using Tri Reagent (Sigma-Aldrich) as recommended. RPAs were performed on 1–20 μg of total RNA using the Riboquant MultiProbe RNase Protection Assay System (BD Biosciences), following manufacturer's instructions. Multiprobe template sets mCK2b, mCK3b, and mCK5 were used. DNA templates were used to synthesize the [^{32}P]UTP (3,000 Ci/mmol or 10 mCi/ml; Amersham Biosciences)-labeled probes in the presence of a GACU pool using a T7 RNA polymerase. Hybridization with 1–20 μg of each target RNA was performed overnight, followed by digestion with RNase A and T1 according to the standard protocol. Samples were treated with a proteinase K–SDS mixture, extracted with chloropan, and precipitated in the presence of ammonium acetate. Samples were run in an acrylamide-urea sequencing gel, next to the labeled probes, at 45 W with 0.5× Tris-borate/EDTA buffer (TBE). The gel was adsorbed to filter paper, dried under vacuum, and exposed on a film (X-AR; Kodak) with an intensifying screen at −70°C. For RT-PCR, 2 μg DNaseI-treated RNA was reverse transcribed with MuLV RT (Roche Diagnostics, Ltd.). Real-time PCR was performed in a rapid thermal cycler system (Lightcycler; Roche Diagnostics, Ltd.) with primers from different exons that generated products of ~200 bp in length. Results for each cytokine are normalized to GAPDH expression and measured in parallel in each sample.

Blockade of TGF-β. In vivo blocking of active TGF-β in tumor challenge mice was performed by administration of 0.5 mg mAb against TGF-β (1D11.16.8; mouse IgG1 hybridoma, purchased from American Type Culture Collection; reference 50), or PBS on days −3, −1, and +1 relative to tumor inoculation and every week after tumor inoculation.

mAb Production. A new panel of mouse CD69-specific mAb was generated by fusion of NS-1 myeloma cells with spleen cells from a CD69-deficient mouse immunized previously three times with mouse 300-19 pre–B cells. Supernatant fluid from hybridoma-containing wells was screened for reactivity with mCD69-transfected Jurkat cells; 42 supernatants reacted with mouse cDNA CD69-transfected Jurkat cells, but not untransfected cells. These hybridomas were selected for characterization and were subcloned twice. Antibody isotypes were determined with a mouse mAb isotyping kit (Boehringer). Antibodies were used either as undiluted culture supernatant or were purified from concentrated supernatants obtained in a CL 350 flask (Integra Biosciences AG) with a protein G column (Amersham Biosciences). Purified mAb were dialyzed extensively against PBS, and their purity was assessed by SDS-PAGE. mAbs were stored at −20°C.

TGF-β and MCP-1 Production and ELISA. For in vitro TGF-β production in NK cells, spleen $DX5^+$ cells of C57BL/6 mice were obtained. 2.5×10^5 NK cells were plated in U-bottomed 96-well plates in 200 μl of serum-free Stem Span (Stem-Cell Technologies Inc.) medium. Purified anti-CD69, clone CD69.2.2 (IgG1-κ), or control mouse IgG1 mAb were added at 10 μg/ml. For cross-linking, $F(ab')_2$ fragments of goat anti–mouse IgG Fc-specific antibody (Jackson ImmunoResearch Laboratories) were added at a final concentration of 20 μg/ml. For in vitro TGF-β production in T lymphocytes, purified $CD3^+$ T cells from single cell suspensions of lymph nodes and spleen of C57BL/6 or BALB/c mice were obtained. For isolation of $CD3^+$ T lymphocytes, cells were incubated with anti–MAC-1 mAb, followed by two panning steps on petri dishes coated with rabbit anti–mouse/rat IgG (DakoCytomation) at 4°C. The average purity of $CD3^+$ cells was >95%, as determined by flow cytometry analysis. T lymphocytes were stimulated (2×10^6 cells/ml) with 1 μg/ml of plate-bound anti-CD3 mAb. Cells were added in 200 μl of serum-free Stem Span medium in flat-bottomed 96-well plates. Anti-CD69, clone CD69.2.2 (IgG1-κ), or control mouse IgG1 mAb were added at 20 μg/ml. For cross-linking, $F(ab')_2$ fragments of goat anti–mouse IgG Fc-specific antibody were added at a final concentration of 20 μg/ml. Cultures were incubated (37°C, 5% CO_2), supernatants were collected after 24, 48, and 72 h, and secreted TGF-β was assayed with a TGF-β1 Emax ImmunoAssay System (Promega) ELISA kit, according to the manufacturer's protocol. To measure MCP-1 production, 1 ml of thioglycollate solution (3% wt/vol; Sigma-Aldrich) was injected intraperitoneally into CD69−/− and WT

mice. Mice were killed 3 d later, and leukocyte infiltrate was recovered by peritoneal lavage using 5 ml of cold RPMI 1640 with 2% FCS. Peritoneal cells were added in 1 ml of complete medium in flat-bottomed 24-well plates and stimulated overnight with 1 μg/ml LPS at 2×10^6 cells/ml. Culture supernatants were collected and MCP-1 was assayed with a mouse MCP-1 OptEIA ELISA Set (BD Biosciences).

Analysis of Cell Viability. T cells were cultured as done for the TGF-β production assay; after 24- and 48-h culture, cell viability was determined by trypan blue addition.

Statistical Analysis. Where indicated, Student's *t*-test for nonpaired data and Mann-Whitney U test were used to calculate statistical significance for difference in a particular measurement between different groups. Statistical significance was set at $P < 0.05$.

Results

Enhanced In Vivo Anti-tumor NK Cell Activity in CD69−/− Mice. NK cells are reported to mediate the immune response to MHC class I^- RMA-S tumor cells, whereas $CD8^+$ CTLs mediate the response to the parental RMA cells bearing MHC class I (22, 23). To evaluate the possible role of CD69 in in vivo anti-tumor function, WT and CD69−/− mice were injected intraperitoneally with RMA-S cells and tumor progression was analyzed (Fig. 1 A). In response to 10^4 RMA-S cells, all WT mice developed tumors by 5 wk after injection, with a detectable weight increase at day 15, whereas only 20% of CD69−/− mice developed detectable tumors even as late as 7 wk (Fig. 1 A). Animals that did not develop tumors were followed for up to 3 mo without any sign of tumor progression. Similar results were observed when mice were subcutaneously injected with 10^5 RMA-S cells (Fig. 1 B), indicating that there are no appreciable differences due to the site of tumor challenge. In contrast, only slight differences were observed in the progression of $H\text{-}2^+$ RMA cell tumors between WT and CD69−/− mice (Fig. 1 C and not depicted), thus suggesting that $CD8^+$ CTLs do not play a major role in the enhanced anti–tumor response observed in CD69−/− mice.

Previous studies showed that NK cells control RMA-S growth in vivo in WT mice (22). To further investigate the involvement of NK cells in the control of RMA-S tumor growth in CD69−/− mice, animals were depleted of NK cells before tumor induction by treatment with anti–asialo-GM1 serum. Injection with either control diluent or anti–asialo-GM1 was initiated on day −1 before tumor challenge and was continued on days +2 and +4 after tumor inoculation. As predicted, tumor growth was observed in all NK cell–depleted mice but in none of the control mice (Fig. 1 D). Anti–asialo-GM1-treated CD69−/− mice developed tumors within the first 10 d after tumor inoculation, which was comparable to the earliest RMA-S tumor

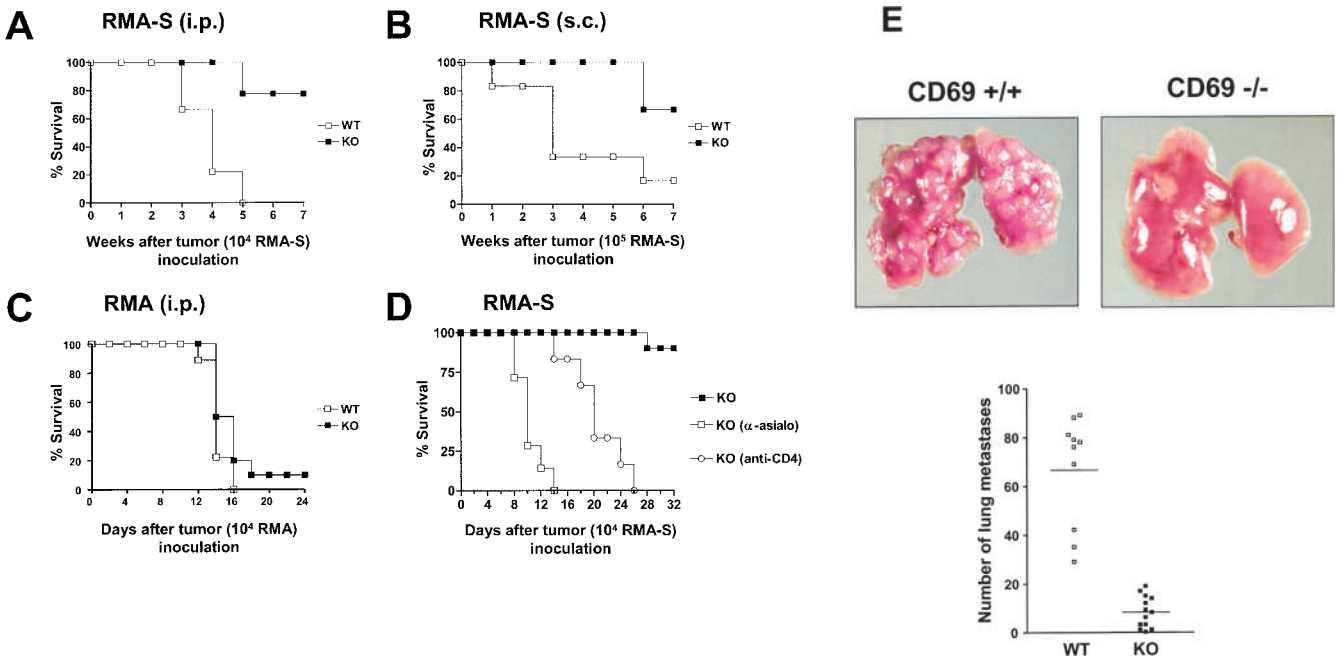

Figure 1. Increased NK anti-tumor activity in CD69−/− mice. Mice were injected intraperitoneally with 10^4 RMA-S (A) or RMA (C) tumor cells. Mice were observed daily for tumor growth up to 12 wk by monitoring body weight and ascites development. Similar results were observed in mice injected subcutaneously with 10^5 RMA-S (B). (A, $n = 9$; B, $n = 6$; C, $n = 9$.) (D) NK or T lymphocytes were depleted from CD69−/− mice before intraperitoneal inoculation with 10^4 RMA-S tumor cells. Mice were treated for NK cell depletion on day −1 (before tumor challenge), and at days +2 and +4 after tumor inoculation with either control diluent or anti–asialo-GM1 antiserum (100 μl/injection). Mice were treated for lymphocyte T $CD4^+$ depletion on day −1 (before tumor challenge), and at days +2 and +4 after tumor inoculation with either GK1.5 anti-CD4 or isotype control mAbs (100 μl/injection). (D, $n = 7$) Results shown are representative of two independent experiments. (E) Photographs are of lungs from CD69−/− and WT mice 2 wk after the challenge with 10^4 RM-1 cells intravenous inoculation (top). One representative mouse out of 10 per group is shown. The number of lung metastases were counted (bottom) and each symbol represents one mouse. Open symbols, WT mice; closed symbols, CD69−/− mice. Results are representative of two independent experiments.

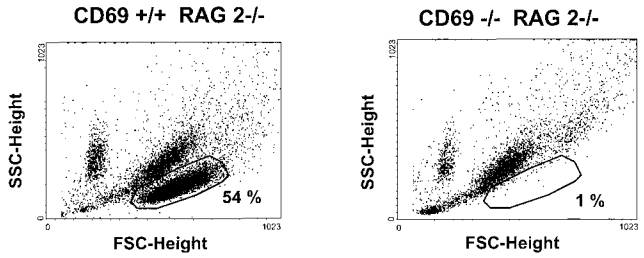

Figure 2. Exacerbated anti–tumor response in CD69−/−RAG-deficient mice. Mice were injected intraperitoneally with 10^6 RMA-S tumor cells. Total unfractionated peritoneal cells from CD69+/+ and CD69−/−−RAG2−/− mice were examined 72 h after tumor inoculation. Forward and scattered FACS® analysis. Marked gates correspond to RMA-S tumor cells. One representative mouse out of 10 per group is shown. Results shown are representative of two independent experiments (n = 8).

development observed in perforin-deficient C57BL/6 mice (22, 24). The depletion of $CD4^+$ or $CD8^+$ lymphocytes in CD69−/− mice increased tumor development but to a lesser extent than NK cell depletion (Fig. 1 D and not depicted). These results indicate that although NK cells are critically involved in RMA-S tumor rejection in CD69−/− mice, T cells also play a role in this process. The increased anti-tumor activity in CD69−/− mice was not restricted to RMA-S cells, because it was also observed after challenge with C57BL/6 syngeneic RM-1 class I^- prostate carcinoma cells. Study of lung metastases in CD69−/− mice compared with WT mice challenged intravenously with 10^4 RM-1 cells showed a greater number of pulmonary metastases in WT mice, whereas CD69−/− mice remained almost free from metastases (Fig. 1 E).

Increased Anti–tumor Response in CD69−/−RAG2−/−-deficient mice. To analyze the contribution of innate immunity to the enhanced anti–tumor response observed in CD69−/− mice, CD69−/−RAG2−/− mice and CD69+/+RAG2−/− mice were injected intraperitoneally with 10^6 RMA-S cells and tumor progression was analyzed (Fig. 2). In response to injection of RMA-S cells, tumor cell overgrowth was observed in all CD69+/+ RAG-deficient mice by 3 d, whereas tumor cell growth was almost completely inhibited in CD69−/− RAG2−/− mice (Fig. 2). Therefore, increased control of RMA-S overgrowth was observed in CD69−/−RAG2−/− mice 3 d after tumor inoculation, and these results are in agreement with the major relevant role of NK cells in MHC class I^- negative tumor suppression in CD69−/− mice.

CD69−/− Mice Show Unaltered NK Cell Function. To assess whether tumor rejection was associated with increased NK cell function, the lytic activity of peritoneal cells of RMA-S–primed CD69−/− and WT mice was determined based on their ability to lyse NK-susceptible YAC-1 tumor cells in vitro. Freshly isolated unfractionated peritoneal cells from RMA-S–inoculated (day 3) CD69−/− mice were more efficient in killing YAC-1 than those from WT mice (Fig. 3 A), thus showing a correlation between the in vivo NK immune response and in vitro NK cytotoxicity in CD69−/− mice. Increased tumor-induced NK cytolytic activity in CD69−/− mice was also observed after challenge with RM-1 prostate carcinoma cells (Fig. 3 B). However, when in vitro NK cell cytolytic assays were performed with purified $DX5^+$ $CD3^-$ NK splenocytes and YAC-1 targets, no differences between CD69−/− and WT mice were observed (Fig. 3 C). Moreover, no differences were found when purified NK cells were expanded by culture in IL-2 and assayed for cytolytic activity (Fig. 3 D). Thus, CD69−/− mice have normal levels of NK activity in the spleen, indicating that the cytolytic potential of CD69−/− NK cells is unaltered by the absence of CD69.

Increased Local NK Cells and T Lymphocyte Accumulation in CD69−/− Mice. To investigate the mechanism accounting for the enhanced anti–tumor response that correlates with the increased cytotoxic activity of unfractionated peritoneal cells, the peritoneum of CD69−/− animals was analyzed. NK cells, T lymphocytes, and total peritoneal

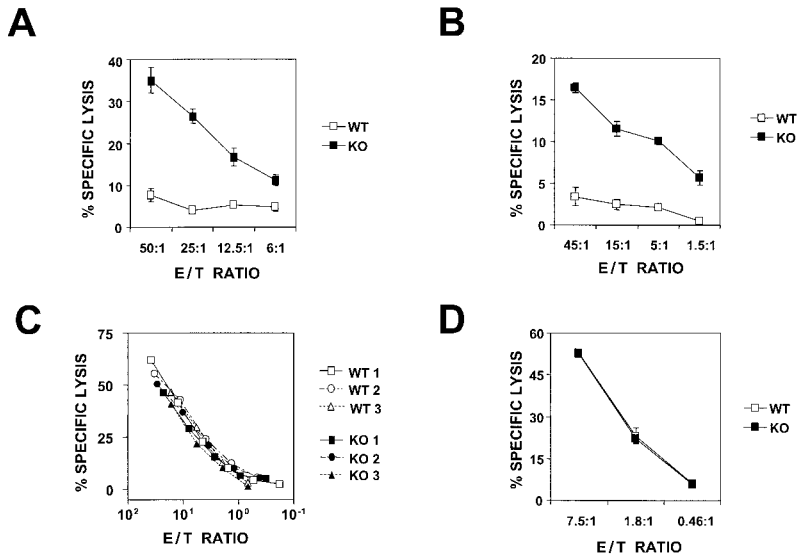

Figure 3. Increased ex vivo NK cytotoxicity in CD69−/− mice. Mice received 10^4 RMA-S (A) or RM-1 cells (B) intraperitoneally 72 h after inoculation, total unfractionated peritoneal cells (A and B) from CD69−/− and WT mice were analyzed for cytotoxicity against YAC target cells. Two animals were used per experimental group (mean ± SE). (C and D) Purified NK cells were used, untreated or treated with IL-2, respectively. (D) Two animals were used per experimental group (mean ± SE). Open symbols, WT; closed symbols, CD69−/−. The results are representative of three similar experiments.

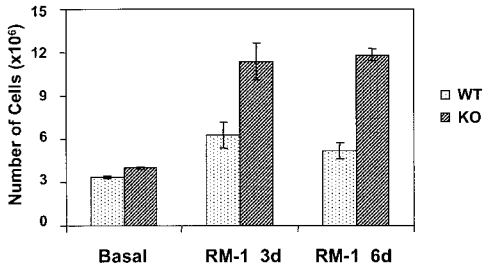

Figure 4. Peritoneal cell accumulation in CD69−/− mice in response to MHC class I⁻ tumor cells. Mice were injected intraperitoneally with PBS or with 10^5 RM-1 cells (n = 7, mice/group). Cells collected from the peritoneal lavage were analyzed by FACS® and a Multisizer cell counter, and total leukocyte numbers ($\times 10^{-6}$) determined at the indicated times.

cells were quantified in mice that were unchallenged or challenged with RM-1 or RMA-S cells. Peritoneal NK cells were defined as staining positive with antibodies DX5 and 2B4 by two color flow cytometry. As shown in Fig. 4 and Table I, the total cellularity in unchallenged peritoneal lavage was moderately increased in CD69−/− mice compared with WT mice. This was likely due to an increase in the number and proportion of lymphocytes; specifically, NK cells and $CD3^+$ T lymphocytes (twofold; Table I A). Upon the RM-1 tumor challenge, the total number of cells recruited to peritoneum in CD69−/− mice was significantly increased compared with WT mice (Fig. 4 and Table I A). This reflects an increase in lymphocyte recruitment; the number of NK cells and $CD3^+$ T lymphocytes was almost threefold higher in CD69-deficient mice compared with WT mice (Fig. 4 and Table I). In contrast, the number of peritoneal $CD5^+B220^+$ B-1 and $CD5^-B220^+$ B-2 lymphocytes was similar in CD69−/− and WT mice, both under basal conditions and after tumor challenge with RM-1 (unpublished data). We detected only slight increases in monocytes and granulocytes in CD69−/− peritoneum compared with WT mice (unpublished data). These data reveal a correlation between the number of NK cells and $CD3^+$ T lymphocytes in the peritoneum of CD69−/− mice and the anti–tumor response. Similar results were observed when mice were intraperitoneally challenged with RMA-S cells (unpublished data). Thus, CD69 does not appear to regulate NK cell cytolytic activity per se, but instead regulates the number of NK cells and $CD3^+$ T lymphocytes recruited to the site of tumor challenge.

The spleen is a lymphoid organ strongly influenced by peritoneal inflammation. Accordingly, at day 6 of tumor challenge, CD69−/− mouse spleens were much enlarged compared with those of WT mice (unpublished data). Spleen cell counts showed a similar trend (Table I), although flow cytometric analyses revealed similar proportions of

Table I. *Basal and RM-1 Challenged*

		A. Peritoneum				
		Total cells[a]	Percent NK cells[b]	Total NKS[c]	Percent $CD3^+$ cells[d]	Total $CD3^+$ cells[e]
		×10⁶		*×10⁴*		*×10⁴*
Basal	WT	3.29 ± 0.08	0.96 ± 0.07	3.15	8.36 ± 1.04	27.5
	KO	4.01 ± 0.12	1.64 ± 0.10	6.57	14.60 ± 0.65	58.54
RM-1 (3 d)	WT	6.24 ± 0.90	2.50 ± 0.21*	15.6	12.75 ± 0.57	79.56
	KO	11.39 ± 1.28	3.51 ± 0.31	39.97	18.42 ± 0.89	209.8

		B. Spleen		
		Basal[f]	RM-1 (3 d)[g]	RM-1 (6 d)[h]
Total cells ($\times 10^6$)	WT	63.78 ± 5.12*	68.4 ± 4.54	88.52 ± 7.09
	KO	96.71 ± 10.94	121.25 ± 11.25	139.87 ± 7.68
Spleen weight (mg)	WT	54.58 ± 2.63	61.85 ± 2.87	89.29 ± 6.61
	KO	75.84 ± 4.81	87.54 ± 4.24	123.67 ± 7.34

Data represents mean ± SE of three independent experiments. P value is $P < 0.005$ for all except asterisk, $P = 0.02$.
[a]Basal, n = 7; RM-1 (3 d), n = 11.
[b]Basal, n = 10; RM-1 (3 d), n = 16.
[c]Total NK = percent NK cells × total cells ($\times 10^6$).
[d]Basal, n = 4; RM-1 (3 d), n = 12.
[e]Total $CD3^+$ cells = percent $CD3^+$ cells × total cells ($\times 10^6$).
[f]Total cells, n = 6; spleen weight, n = 12.
[g]Total cells, n = 4; spleen weight, n = 14.
[h]Total cells, n = 10; spleen weight, n = 10.

$B220^+$, $CD3^+$, and $DX5^+$ spleen lymphocytes in CD69−/− and WT mice (unpublished data). Further analyses using a set of antibodies against different TCR Vβs demonstrated that the T cell expansion was polyclonal (unpublished data). Finally, a moderate but significant increase in spleen size was observed in unchallenged CD69−/− mice (Table I B). Together, these data suggest a role for CD69 as a regulator of lymphocyte accumulation at inflammation sites. This altered homeostasis might occur by modifications of lymphocytes or their microenvironmental milieu.

Normal Trafficking of CD69−/− Lymphocytes. The increased number of lymphocytes in some activated tissues of CD69−/− mice might be due to altered trafficking of activated lymphocytes in the absence of this molecule. To determine a possible role of CD69 in lymphocyte trafficking, we compared the migration of activated $CD4^+$ T lymphocytes from WT mice, expressing high levels of CD69 (unpublished data) and from CD69−/− mice by in vivo cell transfer. Purified $CD4^+$ T cells from CD69−/− and WT mice were PMA-activated for 3 h, introduced into WT recipients, and their distribution was assayed 1 h later (Fig. 5 A). No significant differences in the migration pattern to various organs were observed for both CD69−/− and WT $CD4^+$ T lymphocytes (Fig. 5 A). Almost identical numbers of WT and CD69−/− $CD4^+$ T lymphocytes were also detected in all organs when 24-h migration experiments were performed (Fig. 5 B). Likewise, homing was identical for activated splenic B cells of CD69−/− and WT mice (unpublished data).

Augmented Lymphocyte Survival in CD69−/− Mice. In the periphery, homeostatic mechanisms regulate the expansion and elimination of activated cells (25). To investigate the mechanism of lymphocyte accumulation in CD69−/− mouse spleen and peritoneum, we analyzed immune cell survival in these mice. When peritoneal cell viability was studied in vitro, an increase in cell survival was detected in CD69−/− compared with WT mice (Fig. 6 A). A significant decrease in spontaneous apoptosis (24 h) of spleen lymphocytes from RM-1–challenged CD69−/− (23.36 ± 1.73%, $n = 9$) compared with WT mice (28.89 ± 1.18%, $n = 9$) was detected as reduced DNA content by cell cycle analyses (unpublished data; $P \leq 0.02$). In addition, a significant decrease in spontaneous apoptosis (48 h) of spleen lymphocytes from RM-1–challenged CD69−/− (25.46 ± 0.5%, $n = 6$) compared with WT mice (44.56 ± 1.3%, $n = 6$) was also measured by caspase-3 activation analysis (Fig. 6 B; $P \leq 0.0001$). Likewise, a significant decrease in spontaneous apoptosis (48 h) was observed when caspase-3 activation analyses were performed in $DX5^+$ $CD3^-$ NK splenocytes from RM-1–challenged CD69−/− (36.98 ± 1.5%, $n = 4$) compared with WT mice (49.78 ± 3.9%, $n = 4$; Fig. 6 C, $P \leq 0.02$). Thus, it appears that differences in lymphocyte survival may contribute to the elevated spleen size and cellularity observed in peritoneum of CD69−/− mice.

Decreased TGF-β and Increased Proinflammatory Factors in CD69−/− Mice. The anti–tumor response is orchestrated by a wide array of growth factors and cytokines, and

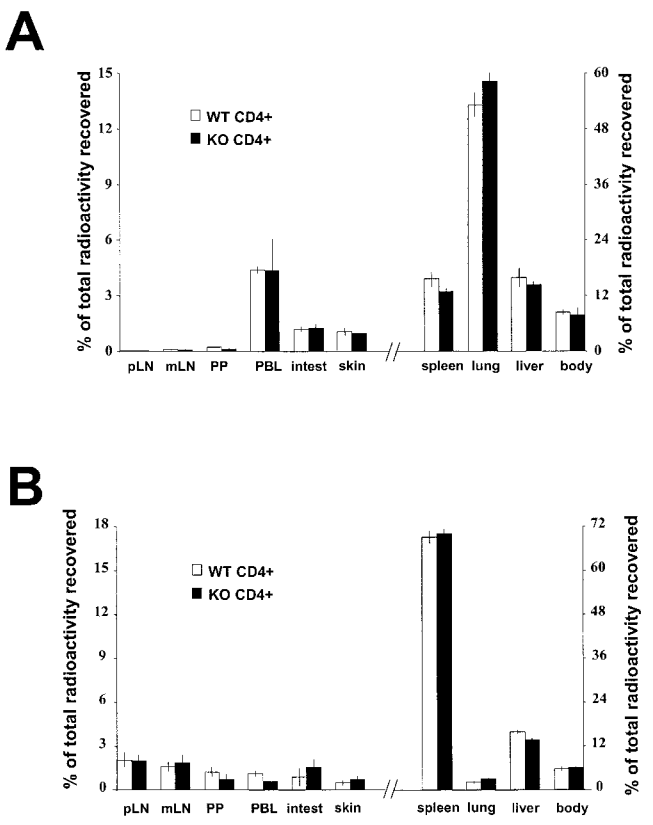

Figure 5. Similar trafficking of activated CD69−/− and WT $CD4^+$ T cells. Short-term (A) and 24-h (B) trafficking patterns of activated CD69−/− and WT $CD4^+$ T cells do not differ. Distribution of radioactivity in various organs at 1 or 24 h, respectively, after intravenous injection of activated ^{51}Cr-labeled $CD4^+$ T cells. Note the numerical scales for organs shown on the right. Four animals were used per experimental group (bars ± SD).

altered expression of these factors may have a major impact on immune responses. Therefore, we analyzed whether the enhanced anti–tumor response of CD69−/− as compared with WT mice is influenced by differences in chemokine and cytokine profiles. Assessment of relative levels of cytokine mRNA was performed by RPA. Analysis of peritoneal cells of RM-1–primed CD69−/− mice showed an increase in MCP-1 (133%), but the chemokines MIP-1α, MIP-1β, IP-10, and eotaxin were unaltered (Fig. 7 A). To further examine MCP-1 production, we tested the ability of LPS-activated peritoneal cells from thioglycollate-treated mice to produce MCP-1; the levels of MCP-1 produced by peritoneal cells from CD69−/− mice were almost three times higher than those of WT mice (Fig. 7 B). In addition, analysis of peritoneal cell RNA of RM-1–challenged CD69−/− showed a change in TGF-β production compared with WT mice. CD69−/− peritoneal cells produced less TGF-β1, -β2, and -β3 transcripts than WT peritoneal cells (Fig. 7 A). The decrease in mRNA levels observed in four separate experiments ranged from 33 ± 5% for TGF-β1 levels to 74 ± 19% for TGF-β3. The decrease in TGF-β2 RNA was sex-

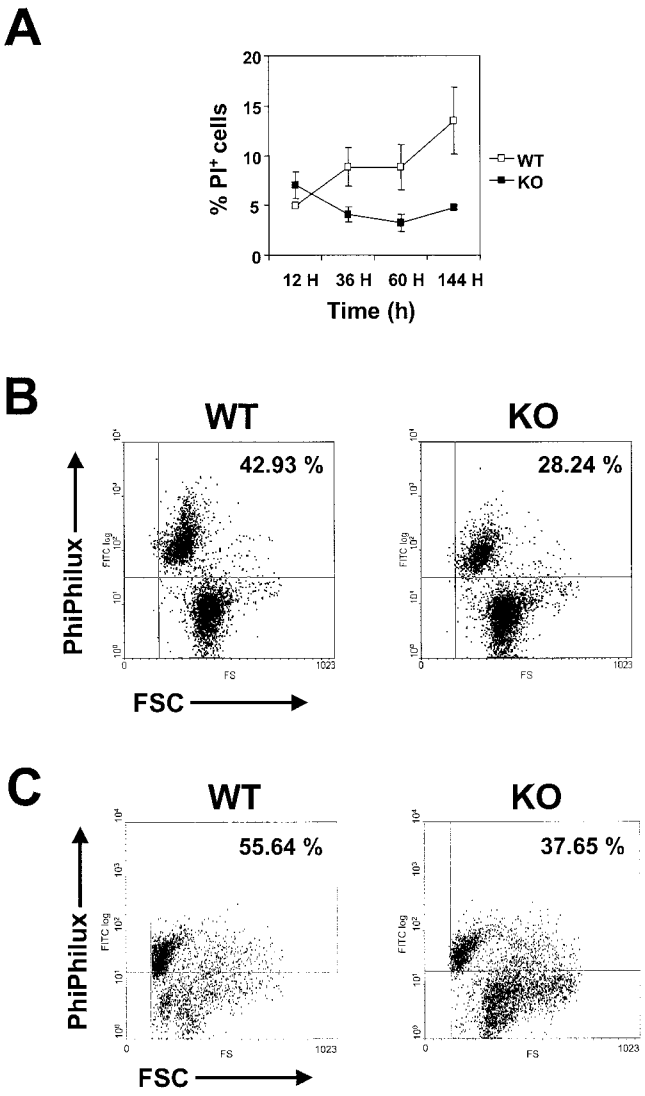

Figure 6. Attenuation of spontaneous cell death of CD69−/− lymphocytes. (A) Unfractionated peritoneal cells of untreated mice were seeded in culture medium and cell survival was measured by PI staining. Values show the percentage of PI^+ cells (mean ± SD; $n = 3$ for each group). Results are representative of three independent experiments. (B) Analysis of intracellular caspase-3 activity of spleen cells from WT (left) and CD69−/− (right) challenge mice (3 d with 10^5 RM-1). Caspase-3 activation was detected with fluorogenic substrate PhiPhiLux-G1D2. PhiPhiLux staining on FL-1 versus forward scatter channels was displayed. (C) After gating on $DX5^+$ cells from spleen, caspase-3 activity was assayed. At least 100,000 events were collected per sample. Experiments were done twice with four and six mice per group; and similar results were obtained.

dependent, varying from 20% for males to 110% for females. Analysis of splenocytes revealed only slight decreases in TGF-β1 and TGF-β3 in CD69−/− mice (unpublished data). Analysis of peritoneal cells of RM-1–primed CD69−/− mice revealed an increase in cytokines IL-12p35 (32–68%), IL-1α (27–64%), IL-1β (32% for males, 294% for females) compared with WT mice (Fig. 7 A). No significant changes in LT-β, IFNγ, MIF, IL-1–Rα, IL-18, eotaxin, MIP-1α, MIP-1β, and IP-10 were found (Fig. 7 A and not depicted). Thus, these results suggest that the immune cells from CD69−/− mice have abnormal chemokine and cytokine expression patterns, with defective synthesis of immunosuppressive factors and increased production of proinflammatory cytokines.

Because innate immunity is highly involved in the increased anti–tumor response observed in CD69−/− mice, we next determined cytokine mRNA levels in purified NK cells and macrophages from RM-1–challenged CD69−/− and WT mice with quantitative real time RT-PCR. These analyses showed a reduction in TGF-β1 and an increase in IL-1β and MCP-1 mRNA levels in both macrophages and NK cells from CD69−/− mice (Fig. 7 C). Therefore, NK cells and macrophages contribute to the observed differences in TGF-β, IL-1β, and MCP-1 levels between WT and CD69−/− mice. These results are in accordance with the proposed role of TGF-β1 as a repressor in anti–tumor response (26, 27). These changes in chemokines and cytokines observed in CD69−/− mice may account for the more potent immune response and the enrichment in T and NK lymphocytes observed in CD69−/− as compared with WT mice.

Effect of TGF-β Blockade in Anti–tumor response in WT Mice. To establish a functional correlation between the reduction in TGF-β levels and the increased anti–tumor response observed in CD69−/− mice, WT mice were treated with a blocking anti–TGF-β mAb. TGF-β blockade with the mAb prevented tumor development compared with the control antibody or carrier (Fig. 8). These results indicate that TGF-β blockade in tumor-challenged mice results in a similar phenotype to that seen in CD69-deficient mice, thus underscoring the diminished production of TGF-β found in CD69−/− mice as the basis for their enhanced anti-tumor immunity.

CD69 Up-regulates TGF-β Secretion. Based on the evidence from CD69−/− mice, CD69 may negatively regulate cell activation through TGF-β. Thus, we examined whether TGF-β is regulated by signaling through CD69 in T and NK cells. CD69 cross-linking induced TGF-β production in purified NK cells (Fig. 9 A), most of them $CD69^+$ (unpublished data). Cross-linked, but not soluble, anti-CD69 (mAb CD69.2.2) induced TGF-β1 synthesis independently of further costimulus (Fig. 9 A and not depicted). In these assays, increased active TGF-β1 correlated with total TGF-β1 synthesis. Next, we analyzed TGF-β1 production in activated T cells. Stimulation with anti-CD3 induced increased CD69 expression by purified spleen T cells of B6 mice (Fig. 9 B). CD69 cross-linking on CD3-activated T cells markedly induced TGF-β production (Fig. 9 C). This effect was not observed using a control isotype-matched antibody (Fig. 9 C), indicating that antibody cross-linking of CD3 alone did not induce TGF-β secretion as described previously (28). Quantification of viable and nonviable cells (Fig. 9 C) at 48 h after cell culture showed a reduction in lymphocyte survival, which correlates with enhanced TGF-β levels. Together these results establish a direct link between CD69 engagement and TGF-β1 synthesis in both NK and T cells, and may ac-

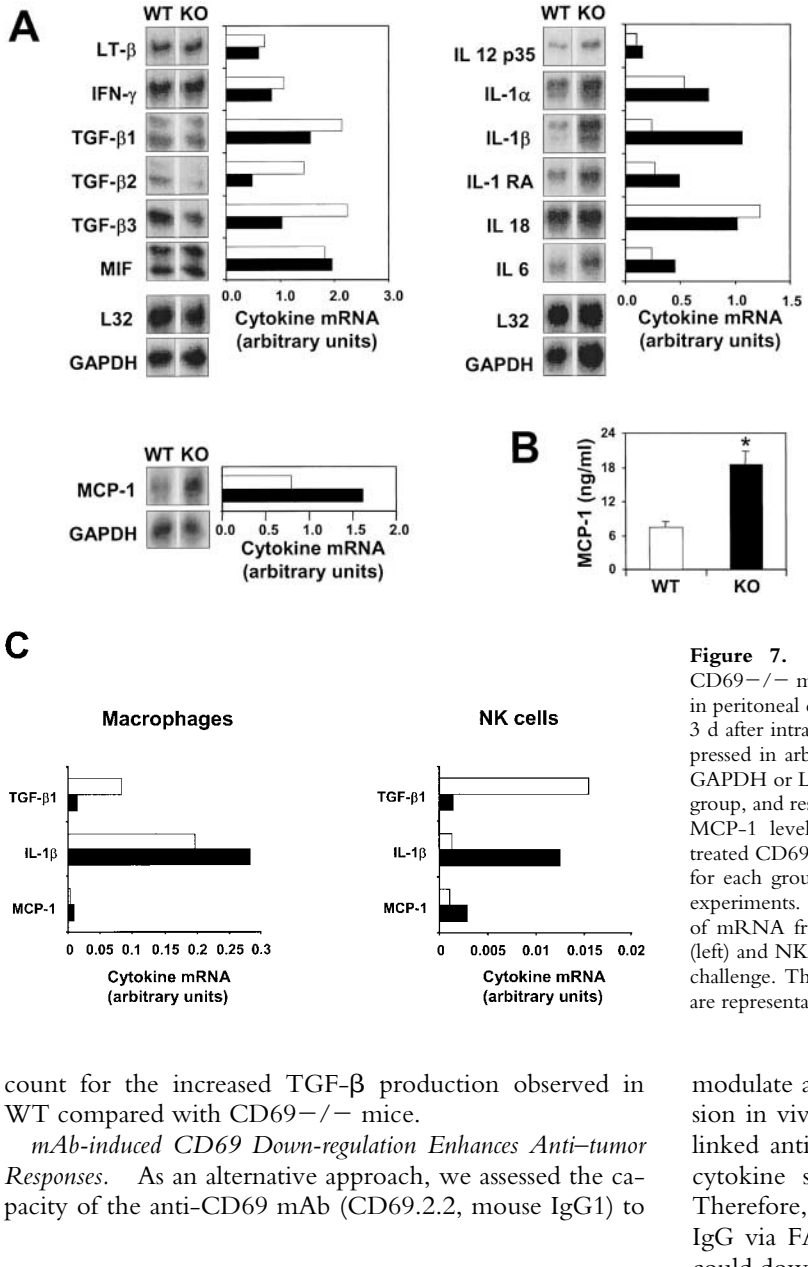

Figure 7. Altered chemokine and cytokine pattern expression in CD69−/− mice. (A) Relative levels of cytokine and chemokine mRNA in peritoneal cells from CD69−/− (■) and WT (□) mice were analyzed 3 d after intraperitoneally inoculation of 10^5 RM-1 cells. Results are expressed in arbitrary densitometric units normalized for the expression of GAPDH or L32 in each sample. Five animals were used per experimental group, and results are representative of four independent experiments. (B) MCP-1 levels in LPS-activated peritoneal cells from thioglycollated-treated CD69−/− and WT mice. Data represent the mean ± SE ($n = 4$ for each group) of one experiment representative of three independent experiments. *, $P < 0.004$. (C) Quantitative real-time RT-PCR analysis of mRNA from CD69−/− and WT purified peritoneal macrophages (left) and NK cells (right) obtained from mice after 6 d of 10^5 i.p. RM-1 challenge. Three animals were used per experimental group, and results are representative of one experiment.

count for the increased TGF-β production observed in WT compared with CD69−/− mice.

mAb-induced CD69 Down-regulation Enhances Anti–tumor Responses. As an alternative approach, we assessed the capacity of the anti-CD69 mAb (CD69.2.2, mouse IgG1) to modulate anti–tumor responses by blocking CD69 expression in vivo. As aforementioned, and in contrast to cross-linked antibodies, soluble CD69.2.2 mAb did not induce cytokine synthesis by $CD69^+$ cells (unpublished data). Therefore, we quantified binding of labeled anti–mouse IgG via FACS® analysis to determine if soluble mAb-2.2 could down-regulate CD69 expression.

A single injection of purified mAb-CD69.2.2 (500 μg i.p. per mouse) completely abolished CD69 expression in both mature and immature hematopoietic cells in central and peripheral lymphoid organs (Fig. 10 A and not depicted), an effect that lasted for more than 15 d. The blockade was specific in that no concomitant changes were detected in the number of cells in lymphoid organs, or in the expression levels of CD3, CD2, CD4, CD8 (Fig. 10 A), IgM, IgD, Ly6G, B220, and CD5 surface molecules (unpublished data). Moreover, mAb-CD69.2.2 did not mediate cell lysis by complement activation and ADCC when tested in vitro (unpublished data). Thus, mAb-CD69.2.2 elicited a remarkably specific down-regulation of CD69 expression in murine cells in vivo while operating as a nondepleting antibody.

To determine whether the mAb-CD69.2.2–induced down-regulation of CD69 expression enhanced the anti–

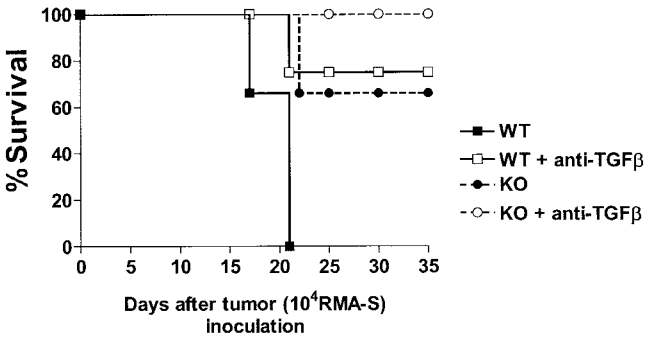

Figure 8. Enhanced anti-tumor activity by blocking anti–TGF-β in WT mice. Survival plot of WT and CD69−/− mice intraperitoneally injected on day 0 with 10^4 RMA-S cells and treated with either 1D11 anti–TGF-β mAb (500 μg/injection) or PBS on days −3 and −1 (before tumor challenge), and at day +1 and every week after tumor inoculation. ($n = 4$). Results shown are representative of two independent experiments.

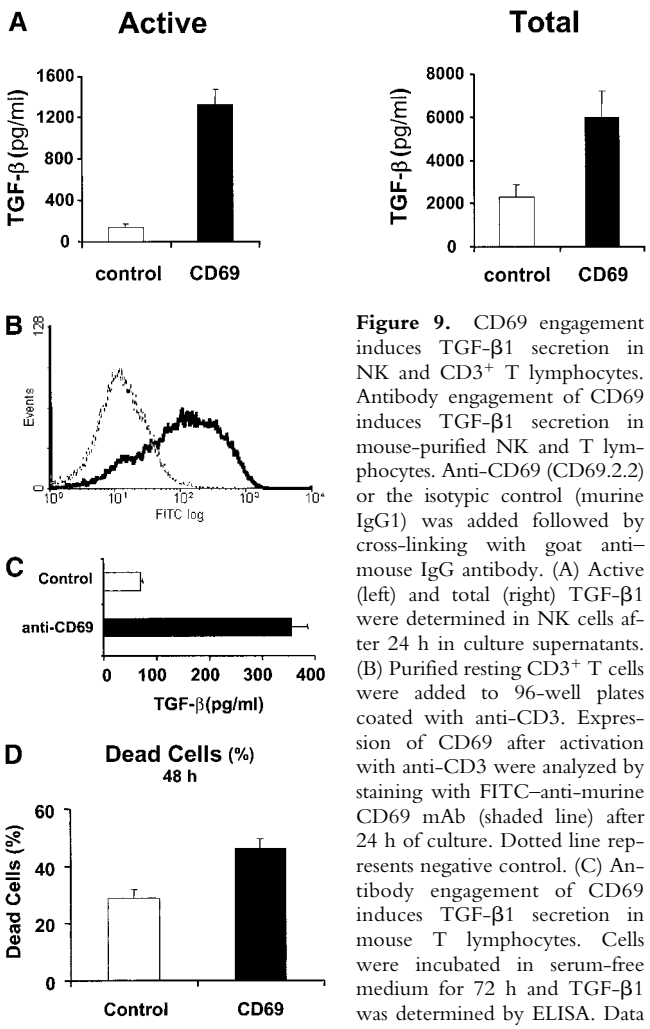

Figure 9. CD69 engagement induces TGF-β1 secretion in NK and $CD3^+$ T lymphocytes. Antibody engagement of CD69 induces TGF-β1 secretion in mouse-purified NK and T lymphocytes. Anti-CD69 (CD69.2.2) or the isotypic control (murine IgG1) was added followed by cross-linking with goat anti–mouse IgG antibody. (A) Active (left) and total (right) TGF-β1 were determined in NK cells after 24 h in culture supernatants. (B) Purified resting $CD3^+$ T cells were added to 96-well plates coated with anti-CD3. Expression of CD69 after activation with anti-CD3 were analyzed by staining with FITC–anti-murine CD69 mAb (shaded line) after 24 h of culture. Dotted line represents negative control. (C) Antibody engagement of CD69 induces TGF-β1 secretion in mouse T lymphocytes. Cells were incubated in serum-free medium for 72 h and TGF-β1 was determined by ELISA. Data are expressed as mean ± SD of replicate wells and are representative of three independent experiments. (D) Cultured cells were removed and trypan blue was added. Dead cells (trypan blue positive) was determined after 48 h of culture. Data represent means of triplicate wells (bars ± SD).

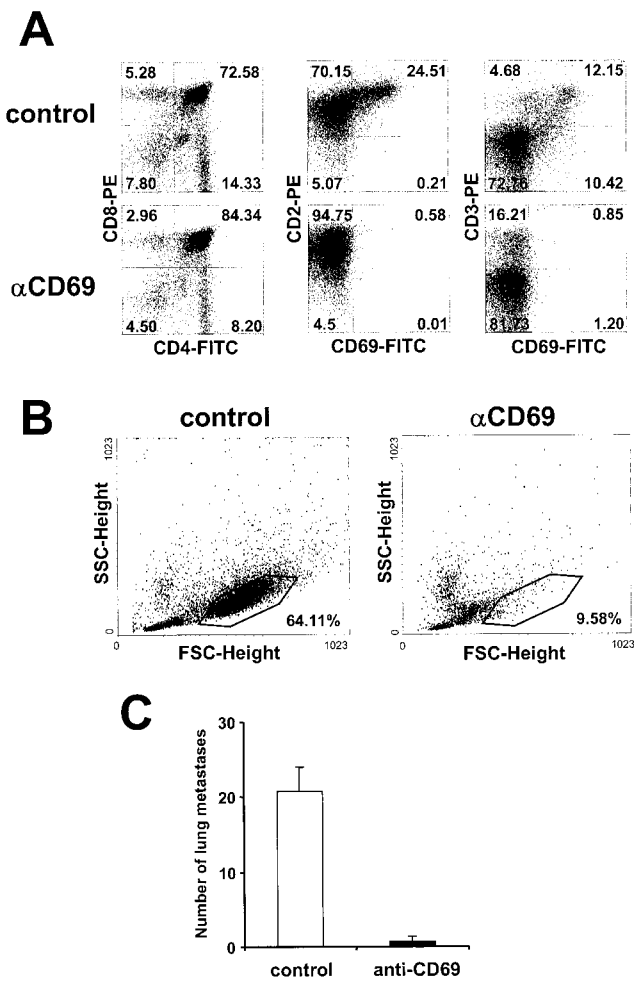

Figure 10. Therapeutic anti-tumor activity of anti-CD69 mAbs. 8-wk-old C57BL/6 mice were treated intraperitoneally with 500 μg anti-CD69.2.2 or with the isotype control (mouse IgG1). (A) Thymocytes were prepared from the treated mice, and were subjected to flow cytometric analysis. Representative profiles of CD4/CD8, CD2/CD69 (10 d after mAb injection), and CD3/CD69 (15 d after mAb injection) are shown with the percentage of cells in each quadrant. (B) Peritoneal cells of WT mice were examined at day 3 after intraperitoneal injection of 10^6 RMA-S tumor cells. Mice were treated with mAb 1 d before tumor inoculation. Cells collected from the peritoneal lavage were analyzed and forward and scattered FACS® analysis is shown. Marked gates correspond to RMA-S tumor cells. (C) Mice were injected intravenously with 10^4 RM-1 and were treated with mAb on day −1 (before tumor challenge). Number of lung metastases was counted 14 d after tumor inoculation. (C) Open bar, control mice; closed bar, anti-CD69 mAb treated WT mice (bars ± SD). Results are representative of two independent experiments ($n = 3$).

tumor response, tumor progression was analyzed in mAb-CD69.2.2 and isotype-control treated WT mice after injections with RMA-S cells (10^6 i.p.). Tumor cell growth was almost completely inhibited in animals treated with mAb-CD69.2.2, whereas control mice presented significant tumor cell overgrowth by 3 d (Fig. 10 B). (In addition, the number of pulmonary metastases was drastically reduced in mAb-CD69.2.2–treated WT mice when compared with isotype-treated controls after challenge with RM-1 cells [10^4 i.v.; Fig. 10 C].) Treatment with anti-CD69 antibodies inhibited (both) RMA-S overgrowth (and RM-1–induced pulmonary metastases), thus supporting our working hypothesis that CD69 blockade enhances anti–tumor responses.

Discussion

We found that CD69-deficient mice exhibit a potent immune response against tumor cells, and that this phenomenon is related to an altered balance in cellular and soluble effector components. These findings support a novel role for CD69 as a negative regulator of the immune response. Previous in vitro studies proposed that CD69 acts as a stimulatory receptor for NK cells that can be blocked by CD94 (15, 29). Earlier in vitro studies suggested that CD69 is a proactivatory molecule in all leukocytes, including NK cells (3, 11). Our findings here nonetheless indicate that CD69 exerts a down-regulatory role in vivo in the immune system.

Studies of mice deficient in any of several molecules (IL-2, IL-2R, CD45, CTLA-4, or TGF-β) have shown that the uncontrolled size and content of the immune compartment causes enhanced immune reactivity (30–34). In these studies, the roles of T cells and T cell–derived cytokines have been examined exhaustively, but the role of NK cells has not. Our data show that an increase in the size of the NK and T lymphocyte compartments enhances immune reactivity toward tumor cells. This finding is consistent with a unique functional role for NK cells' and T lymphocytes' interaction in the immune response as the primary source of immunoregulatory cytokines (35, 36).

The tumoricidal activity of lymphocytes is dependent on their activation state, the effector: target cell ratio, and the susceptibility of the tumor targets. Our data show that the immune response and survival to challenge with MHC class I–deficient tumor cells (RMA-S and RM-1) is dramatically increased in CD69−/− mice, and that this phenomenon is not comparably observed when the same tumor cells expressing MHC class I molecules (RMA) are used. In the MHC class I–deficient tumor models used, $CD3^-$ NK cells were the primary effector cells (22, 23), as demonstrated by in vivo NK cell depletion experiments and the increased anti–tumor response of CD69−/− RAG-deficient mice. This concurs with the finding of enhanced NK cytotoxic activity in unfractionated peritoneal cells from CD69−/− mice. However, no differences in the cytotoxic activity of purified splenic $DX5^+$ NK cells or lymphokine-activated killer cells were detected between WT and CD69−/− mice.

Increased NK cell number at the site of tumor inoculation seems to account for the increased NK cytotoxic activity. An increased NK cell population showing normal cytotoxic activity was reported in CD45−/− mice (34). In addition, increased T lymphocyte representation in peritoneal cells of CD69−/− mice, as well as T cell depletion experiments, suggest that these cells are also involved in tumor growth control, although to a lesser extent than NK cells. Although the results in RAG-2−/− mice showed T lymphocytes are not required for the increased anti–tumor response observed in this in vivo experimental system, these data are not directly comparable to those obtained in RAG-2+/+ mice because lymphocyte-deficient mice have major differences in cell homeostasis as compared with normal control mice. Our data are thus compatible with both NK and T lymphocytes participating in the augmented tumor growth control in CD69−/− mice. It is feasible that T cell–derived cytokines contribute to the increased NK anti–tumor response seen in CD69−/− mice, as the tumor cells studied are not sensitive to lysis by CTLs. Multiple interactions between NK and T cells have been reported. In this regard, the critical role of $CD4^+$ T cells in the rejection of MHC class I^- tumors has been demonstrated previously (37). Likewise, it has been shown that NK and $CD8^+$ T cells interaction results in TGF-β generation (36).

After activation, lymphocytes display profound alterations in their in vivo homing behavior (38). Because CD69 becomes up-regulated on T cells with a similar kinetics as traffic changes occur, it seemed reasonable that CD69 may have a role in retargeting lymphocytes to other compartments upon activation. Comparison of CD69−/− and WT lymphocytes nonetheless showed no significant differences in the trafficking to various body sites. Thus, it is unlikely that the accumulation of lymphocytes observed in spleen and peritoneum of CD69−/− mice is due to defects in trafficking to competing organs. Alternatively, the changes in cellularity at these sites in untreated CD69−/− mice, and especially in CD69−/− mice inoculated with tumor cells, might be caused by an altered host lymphocyte turnover. Therefore, we tested whether the increased cell numbers in CD69−/− mice might be due to alterations in the fate of cells. Peritoneal cell and splenocyte survival was increased in CD69−/− compared with WT mice, and cell cycle and caspase-3 activity analysis revealed reduced apoptosis in CD69−/− cells. Several in vitro inducers of different apoptotic routes in lymphocytes had similar effects when WT and CD69−/− mice were compared (unpublished data). We previously used a specific peptide to induce proliferation in a TCR transgenic model (4) and showed that lymphocyte proliferation was not altered in CD69-deficient mice. Therefore, the finding of diminished lymphocyte death, coupled with the fact that a high proportion of activated lymphocytes migrating through the body normally die within 24 h (~70%; reference 39) may account, at least in part, for the increased lymphocyte population found in activated locations in CD69−/− mice. The anti-tumor immune response is associated with increased spleen size. In this regard, an enlargement of spleen size, more accentuated in tumor-challenged mice, has been observed in CD69−/− as compared with WT mice. Nevertheless, as reported previously (4), similar splenic cell subsets were detected in CD69−/− and WT mice. However, this analysis did not include a careful examination of subpopulations such as the late immune response subpopulation described recently (40). Our work on the distribution of activated lymphocytes in $CD69^{-/-}$ mice agrees with that of others, in that reduced cell death accounts for preferential tissue distribution of activated T cells (41).

Chemokines orchestrate the migration of immune cells at different stages of maturation and activation. Several papers have suggested that the innate response to tumors is regulated by a cytokine/chemokine network produced by interaction of antigen-presenting cells, NK cells, and stromal elements. In this regard, various chemokines are known to have anti-tumor activity(16), and enhancing activity of lymphocytes by MCP-1 on cytotoxicity, migration, and tumor suppression has been reported (42, 43). Our results show that MCP-1 production of in vitro–activated peritoneal cells and MCP-1α mRNA levels in the tumor challenged peritoneal cavity from CD69−/− mice are increased compared with WT mice, possibly explaining the increased influx of immune cells and antitumor activity in these animals.

The TGF-β family of cytokines is involved in cell growth regulation and apoptosis (44). Lymphoid cells pro-

duce TGF-β, and the critical anti-inflammatory role of this cytokine has been demonstrated in mice lacking TGF-β1 and TGF-β signaling in T cells, which develop inflammatory and autoimmune disorders, respectively (45). TGF-β has an important immunosuppressive role in that it inhibits anti-tumor immune response. Recently, it has been reported that blockade of TGF-β signaling in T cells enhances anti-tumor immunity by facilitating an expansion of tumor-specific $CD8^+$ T cells (27). The analysis of cells involved in tumor rejection in CD69−/− mice showed a decrease in TGF-β mRNA synthesis, which appears to be associated with an increased production of MCP-1 and proinflammatory cytokines such as IL-1α, IL-1β, and IL-12. Moreover, in vivo blockade of TGF-β in WT mice caused an increase in anti–tumor responses comparable to that detected in CD69−/− mice, indicating that the diminished production of TGF-β found in CD69−/− mice is a key factor for their enhanced anti-tumor immunity. Thus, and although it is possible that CD69 might signal TGF-β and proinflammatory cytokines independently, the increase in proinflammatory cytokines in CD69−/− mice might be subsequent to the decrease in TGF-β secretion as TGF-β inhibits proinflammatory cytokine secretion.

It is well-known that TGF-β inhibits T cell proliferation, differentiation, and CTL responses (46, 47). On the other hand, MCP-1 enhances lymphocyte migration and cytotoxicity (43, 48). The combination of increased synthesis of MCP-1 and proinflammatory cytokines and decreased TGF-β production may lead to enhanced T and NK cell responses, accounting for the increased tumor surveillance in CD69−/− mice. Further work is necessary to investigate the role of CD69 in cytokine and chemokine production in different cell subsets.

Our data on cytokine synthesis suggested that CD69-mediated signaling was linked to TGF-β gene expression, and this linkage was confirmed by CD69 cross-linking. Because CD69 engagement induces substantial levels of TGF-β, and this cytokine is a potent inhibitor of lymphocyte-mediated responses, this finding has implications for our understanding of in vivo CD69 function. It is reasonable to envision that TGF-β may play a role in suppression of lymphocyte activation initiated by CD69 interaction, and that elimination of CD69 results in a partial reduction in TGF-β and augmented production of proinflammatory cytokines and chemokines, which may account for the enhanced anti-tumor immune response observed in CD69−/− mice. The increased survival of splenocytes and peritoneal immune cells in CD69−/− mice may be related to defective TGF-β production, and therefore to a diminution in proapoptotic TGF-β stimuli (44). Conversely, increased TGF-β production may be consequence to increased cell apoptosis due to TGF-β released by dying cells (49). Alternatively, the changes in TGF-β secretion and apoptotic processes might be independently induced through CD69 signaling. Consistent with this, TGF-β secretion was not detected in nonactivated cell culture supernatants, although differences in spontaneous apoptosis were observed (unpublished data). In addition, our previous observations of an alteration in the pre–B cell stage of B cell development and an enhancement of T cell–dependent IgG isotype-specific responses in CD69−/− mice (4) are in agreement with the role of TGF-β in B cell differentiation and immunoglobulin production (19). Nevertheless, study of TGF-β production during B cell ontogeny and antigen-dependent immune responses in T cells has not yet been performed in CD69−/− mice. Thus, CD69 expression and interaction with its putative ligand may contribute to negative regulation of the immune response, and to suppression of the inflammatory response. This work significantly contributes to understand the role of CD69 in vivo, revealing its function as an immunomodulatory molecule through the production of TGF-β. In this regard, anti-CD69 antibody treatment in WT mice induced a deficiency in CD69 expression that resulted in augmented anti–tumor response, further supporting evidence that a physiological function of CD69 as a anti-tumor repressor. These results showed the possibility of a novel approach for the therapy of tumors and other immune-mediated diseases by targeting CD69. We are currently studying the mechanisms of action of anti-CD69 mAbs treatment in the control of metastasis and tumor growth. Future work is needed to define the molecular basis of anti-CD69 tumor therapy.

We are grateful to Drs. M. Krangel and R. Amaro for excellent critical reading of the manuscript, Drs. A. Arroyo, R. Castaño, J.V. Planas, and L. del Peso for helpful discussion, Dr. A. Justel for statistical advice, and C. Mark for editorial assistance. We also thank L. Gómez, S. March, and P. Pallarés for their technical assistance, and T. Cueva for maintaining the mouse colony.

This work was supported by grants SAF 99/0034-C01 and C02 from the Spanish Ministerio de Educacion y Cultura. The Department of Immunology and Oncology was founded and is supported by the Spanish Council for Scientific Research and the Pharmacia Corporation. D. Sancho was supported by a grant BEFI 01/9191 from the Instituto de Salud Carlos III (Ministerio de Sanidad y Consumo).

Submitted: 5 August 2002
Revised: 7 February 2003
Accepted: 24 February 2003

References

1. Sanchez-Mateos, P., and F. Sanchez-Madrid. 1991. Structure-function relationship and immunochemical mapping of external and intracellular antigenic sites on the lymphocyte activation inducer molecule, AIM/CD69. *Eur. J. Immunol.* 21:2317–2325.
2. Sant'Angelo, D.B., B. Lucas, P.G. Waterbury, B. Cohen, T. Brabb, J. Goverman, R.N. Germain, and C.A. Janeway, Jr. 1998. A molecular map of T cell development. *Immunity.* 9:179–186.
3. Testi, R., D. D'Ambrosio, R. De Maria, and A. Santoni. 1994. The CD69 receptor: a multipurpose cell-surface trigger for hematopoietic cells. *Immunol. Today.* 15:479–483.
4. Lauzurica, P., D. Sancho, M. Torres, B. Albella, M. Marazuela, T. Merino, J.A. Bueren, A.C. Martinez, and F. Sanchez-Madrid. 2000. Phenotypic and functional characteristics of hematopoietic cell lineages in CD69-deficient mice. *Blood.* 95:2312–2320.

5. Testi, R., J.H. Phillips, and L.L. Lanier. 1989. T cell activation via Leu-23 (CD69). *J. Immunol.* 143:1123–1128.
6. Lopez-Cabrera, M., E. Munoz, M.V. Blazquez, M.A. Ursa, A.G. Santis, and F. Sanchez-Madrid. 1995. Transcriptional regulation of the gene encoding the human C-type lectin leukocyte receptor AIM/CD69 and functional characterization of its tumor necrosis factor-alpha-responsive elements. *J. Biol. Chem.* 270:21545–21551.
7. Laffon, A., R. Garcia-Vicuna, A. Humbria, A.A. Postigo, A.L. Corbi, M.O. de Landazuri, and F. Sanchez-Madrid. 1991. Upregulated expression and function of VLA-4 fibronectin receptors on human activated T cells in rheumatoid arthritis. *J. Clin. Invest.* 88:546–552.
8. Tough, D.F., S. Sun, and J. Sprent. 1997. T cell stimulation in vivo by lipopolysaccharide (LPS). *J. Exp. Med.* 185:2089–2094.
9. Santis, A.G., M.R. Campanero, J.L. Alonso, A. Tugores, M.A. Alonso, E. Yague, J.P. Pivel, and F. Sanchez-Madrid. 1992. Tumor necrosis factor-alpha production induced in T lymphocytes through the AIM/CD69 activation pathway. *Eur. J. Immunol.* 22:1253–1259.
10. Santis, A.G., M.R. Campanero, J.L. Alonso, and F. Sanchez-Madrid. 1992. Regulation of tumor necrosis factor (TNF)-alpha synthesis and TNF receptors expression in T lymphocytes through the CD2 activation pathway. *Eur. J. Immunol.* 22:3155–3160.
11. Cebrian, M., E. Yague, M. Rincón, M. Lopez-Botet, and F. Sánchez-Madrid. 1988. Triggering of T cell proliferation through AIM, an activation inducer molecule expressed on activated human lymphocytes. *J. Exp. Med.* 168:1624–1637.
12. Sancho, D., A.G. Santis, J.L. Alonso-Lebrero, F. Viedma, R. Tejedor, and F. Sanchez-Madrid. 2000. Functional analysis of ligand-binding and signal transduction domains of CD69 and CD23 C-type lectin leukocyte receptors. *J. Immunol.* 165: 3868–3875.
13. Gerosa, F., M. Scardoni, M. Tommasi, C. Benati, L. Snelli, G. Gandini, M. Libonati, G. Tridente, and G. Carra. 1991. Interferon alpha induces expression of the CD69 activation antigen in human resting NK cells, while interferon gamma and tumor necrosis factor alpha are ineffective. *Int. J. Cancer.* 48:473–475.
14. Borrego, F., J. Pena, and R. Solana. 1993. Regulation of CD69 expression on human natural killer cells: differential involvement of protein kinase C and protein tyrosine kinases. *Eur. J. Immunol.* 23:1039–1043.
15. Moretta, A., A. Poggi, D. Pende, G. Tripodi, A.M. Orengo, N. Pella, R. Augugliaro, C. Bottino, E. Ciccone, and L. Moretta. 1991. CD69-mediated pathway of lymphocyte activation: anti-CD69 monoclonal antibodies trigger the cytolytic activity of different lymphoid effector cells with the exception of cytolytic T lymphocytes expressing T cell receptor α/β. *J. Exp. Med.* 174:1393–1398.
16. Van Coillie, E., J. Van Damme, and G. Opdenakker. 1999. The MCP/eotaxin subfamily of CC chemokines. *Cytokine Growth Factor Rev.* 10:61–86.
17. Nagai, M., and T. Masuzawa. 2001. Vaccination with MCP-1 cDNA transfectant on human malignant glioma in nude mice induces migration of monocytes and NK cells to the tumor. *Int. Immunopharmacol.* 1:657–664.
18. Gu, L., B. Rutledge, J. Fiorillo, C. Ernst, I. Grewal, R. Flavell, R. Gladue, and B. Rollins. 1997. In vivo properties of monocyte chemoattractant protein-1. *J. Leukoc. Biol.* 62:577–580.
19. Letterio, J.J., and A.B. Roberts. 1998. Regulation of immune responses by TGF-beta. *Annu. Rev. Immunol.* 16:137–161.
19a. Hodge, G., R. Flower, and P. Han. 1999. Effect of factor VIII concentrate on leucocyte cytokine production: characterization of TGF-beta as an immunomodulatory component in plasma-derived factor VIII concentrate. *Br. J. Haematol.* 106:784–791,
20. Freedman, R.S., A.P. Kudelka, J.J. Kavanagh, C. Verschraegen, C.L. Edwards, M. Nash, L. Levy, E.N. Atkinson, H.Z. Zhang, B. Melichar, et al. 2000. Clinical and biological effects of intraperitoneal injections of recombinant interferon-gamma and recombinant interleukin 2 with or without tumor-infiltrating lymphocytes in patients with ovarian or peritoneal carcinoma. *Clin. Cancer Res.* 6:2268–2278.
21. Screpanti, V., R.P. Wallin, H.G. Ljunggren, and A. Grandien. 2001. A central role for death receptor-mediated apoptosis in the rejection of tumors by NK cells. *J. Immunol.* 167: 2068–2073.
22. Smyth, M.J., J.M. Kelly, A.G. Baxter, H. Korner, and J.D. Sedgwick. 1998. An essential role for tumor necrosis factor in natural killer cell–mediated tumor rejection in the peritoneum. *J. Exp. Med.* 188:1611–1619.
23. Smyth, M.J., M. Taniguchi, and S.E. Street. 2000. The anti-tumor activity of IL-12: mechanisms of innate immunity that are model and dose dependent. *J. Immunol.* 165:2665–2670.
24. Smyth, M.J., and R.W. Johnstone. 2000. Role of TNF in lymphocyte-mediated cytotoxicity. *Microsc. Res. Tech.* 50: 196–208.
25. Krammer, P.H. 2000. CD95's deadly mission in the immune system. *Nature.* 407:789–795.
26. Muraoka, R.S., N. Dumont, C.A. Ritter, T.C. Dugger, D.M. Brantley, J. Chen, E. Easterly, L.R. Roebuck, S. Ryan, P.J. Gotwals, V. Koteliansky, C.L. Arteaga. 2002. Blockade of TGF-beta inhibits mammary tumor cell viability, migration, and metastases. *J. Clin. Invest.* 109:1533–1536.
27. Gorelik, L., and R.A. Flavell. 2001. Immune-mediated eradication of tumors through the blockade of transforming growth factor-beta signaling in T cells. *Nat. Med.* 7:1118–1122.
28. Chen, W., M.E. Frank, W. Jin, and S.M. Wahl. 2001. TGF-beta released by apoptotic T cells contributes to an immunosuppressive milieu. *Immunity.* 14:715–725.
29. Zingoni, A., G. Palmieri, S. Morrone, M. Carretero, M. Lopez-Botet, M. Piccoli, L. Frati, and A. Santoni. 2000. CD69-triggered ERK activation and functions are negatively regulated by CD94/NKG2-A inhibitory receptor. *Eur. J. Immunol.* 30:644–651.
30. Sadlack, B., H. Merz, H. Schorle, A. Schimpl, A.C. Feller, and I. Horak. 1993. Ulcerative colitis-like disease in mice with a disrupted interleukin-2 gene. *Cell.* 75:253–261.
31. Suzuki, H., T.M. Kundig, C. Furlonger, A. Wakeham, E. Timms, T. Matsuyama, R. Schmits, J.J. Simard, P.S. Ohashi, H. Griesser, et al. 1995. Deregulated T cell activation and autoimmunity in mice lacking interleukin-2 receptor beta. *Science.* 268:1472–1476.
32. Tivol, E.A., F. Borriello, A.N. Schweitzer, W.P. Lynch, J.A. Bluestone, and A.H. Sharpe. 1995. Loss of CTLA-4 leads to massive lymphoproliferation and fatal multiorgan tissue destruction, revealing a critical negative regulatory role of CTLA-4. *Immunity.* 3:541–547.
33. Willerford, D.M., J. Chen, J.A. Ferry, L. Davidson, A. Ma, and F.W. Alt. 1995. Interleukin-2 receptor alpha chain regulates the size and content of the peripheral lymphoid com-

partment. *Immunity*. 3:521–530.
34. Yamada, H., K. Kishihara, Y.Y. Kong, and K. Nomoto. 1996. Enhanced generation of NK cells with intact cytotoxic function in CD45 exon 6-deficient mice. *J. Immunol.* 157: 1523–1528.
35. Cooper, M.A., T.A. Fehniger, S.C. Turner, K.S. Chen, B.A. Ghaheri, T. Ghayur, W.E. Carson, and M.A. Caligiuri. 2001. Human natural killer cells: a unique innate immunoregulatory role for the CD56(bright) subset. *Blood*. 97:3146–3151.
36. Gray, J.D., M. Hirokawa, and D.A. Horwitz. 1994. The role of transforming growth factor beta in the generation of suppression: an interaction between CD8+ T and NK cells. *J. Exp. Med*. 180:1937–1942.
37. Levitsky, H.I., A. Lazenby, R.J. Hayashi, D.M. Pardoll. 1994. In vivo priming of two distinct antitumor effector populations: the role of MHC class I expression. *J. Exp. Med*. 179: 1215–1224.
38. Hamann, A., K. Klugewitz, F. Austrup, and D. Jablonski-Westrich. 2000. Activation induces rapid and profound alterations in the trafficking of T cells. *Eur. J. Immunol*. 30:3207–3218.
39. Bode, U., C. Duda, F. Weidner, M. Rodriguez-Palmero, K. Wonigeit, R. Pabst, and J. Westermann. 1999. Activated T cells enter rat lymph nodes and Peyer's patches via high endothelial venules: survival by tissue-specific proliferation and preferential exit of CD8+ T cell progeny. *Eur. J. Immunol*. 29:1487–1495.
40. Monroe, R.J., K.J. Seidl, F. Gaertner, S. Han, F. Chen, J. Sekiguchi, J. Wang, R. Ferrini, L. Davidson, G. Kelsoe, and F.W. Alt. 1999. RAG2:GFP knockin mice reveal novel aspects of RAG2 expression in primary and peripheral lymphoid tissues. *Immunity*. 11:201–212.
41. Westermann, J., and U. Bode. 1999. Distribution of activated T cells migrating through the body: a matter of life and death. *Immunol. Today*. 20:302–306.
42. Taub, D.D., J.R. Ortaldo, S.M. Turcovski-Corrales, M.L. Key, D.L. Longo, and W.J. Murphy. 1996. Beta chemokines costimulate lymphocyte cytolysis, proliferation, and lymphokine production. *J. Leukoc. Biol*. 59:81–89.
43. Nokihara, H., H. Yanagawa, Y. Nishioka, S. Yano, N. Mukaida, K. Matsushima, and S. Sone. 2000. Natural killer cell-dependent suppression of systemic spread of human lung adenocarcinoma cells by monocyte chemoattractant protein-1 gene transfection in severe combined immunodeficient mice. *Cancer Res*. 60:7002–7007.
44. Massague, J., S.W. Blain, and R.S. Lo. 2000. TGFbeta signaling in growth control, cancer, and heritable disorders. *Cell*. 103:295–309.
45. Shull, M.M., I. Ormsby, A.B. Kier, S. Pawlowski, R.J. Diebold, M. Yin, R. Allen, C. Sidman, G. Proetzel, D. Calvin, et al. 1992. Targeted disruption of the mouse transforming growth factor-beta 1 gene results in multifocal inflammatory disease. *Nature*. 359:693–699.
46. Gorelik, L., and R.A. Flavell. 2000. Abrogation of TGFbeta signaling in T cells leads to spontaneous T cell differentiation and autoimmune disease. *Immunity*. 12:171–181.
47. Kehrl, J.H., L.M. Wakefield, A.B. Roberts, S. Jakowlew, M. Alvarez-Mon, R. Derynck, M.B. Sporn, and A.S. Fauci. 1986. Production of transforming growth factor β by human T lymphocytes and its potential role in the regulation of T cell growth. *J. Exp. Med*. 163:1037–1050.
48. Loetscher, P., M. Seitz, I. Clark-Lewis, M. Baggiolini, and B. Moser. 1996. Activation of NK cells by CC chemokines. Chemotaxis, Ca2+ mobilization, and enzyme release. *J. Immunol*. 156:322–327.
49. Chen, W., M.E. Frank, W. Jin, and S.M. Wahl. 2001. TGF-beta released by apoptotic T cells contributes to an immunosuppressive milieu. *Immunity*. 14:715–725.
50. Dasch, J.R., D.R. Pace, W. Waegell, D. Inenaga, and L. Ellingsworth. 1989. Monoclonal antibodies recognizing transforming growth factor-beta. Bioactivity neutralization and transforming growth factor beta 2 affinity purification. *J. Immunol*. 142:1536–1541.